

Supporting Information

Tumor microenvironment responsive T_1 - T_2 dual-mode contrast agent Fe_3O_4 @ZIF-8-Zn-Mn nanoparticles for *in vivo* magnetic resonance imaging

Minmin Liang,^a Weixiu Zhou,^a Jutian Zheng,^a Jiaomin Lin,^{*a, b} Lu An,^a and Shiping Yang^{*a}

a The Key Laboratory of Resource Chemistry of the Ministry of Education, the Shanghai Key Laboratory of Rare Earth Functional Materials, and the Shanghai Municipal Education Committee Key Laboratory of Molecular Imaging Probes and Sensors, Shanghai Normal University, Shanghai, 200234 China

* Corresponding authors

Email-addresses: linjm@shnu.edu.cn (J.M. Lin) shipingy@shnu.edu.cn (S.P. Yang)

Preparation of oil-soluble Fe₃O₄ NPs. Oil-soluble Fe₃O₄ NPs (Fe₃O₄-OA) were synthesized according to a previous reported approach with a slightly modification. Firstly, we set up the high-temperature pyrolysis device: A 100 mL three-necked flask was putted on a high-temperature-resistant stirrer with a thermometer, an air condenser and a long needle for nitrogen at the three ports to ensure good air-tightness of the device. Subsequently, 35 mL of oleylamine was put into the three-necked flask, and stirred at 200°C for 2 h under a nitrogen atmosphere. After that, the nitrogen flow was stopped and a nitrogen balloon was placed on the rack. The device was heated to 300 °C to remove residual moisture and oxygen. Then, 2,4-Fe(III) 2,4-glutarate dissolved in 4 mL NMP and 6 mL OA were added into the device with 10 mL syringe. After reaction at 300 °C for 10 min, the reaction was stopped. After the temperature was returned to room temperature, the Fe₃O₄-OA NPs were collected by centrifugation and washed with ethanol and n-hexane (the volume ratio of ethanol and n-hexane is 2:1, 10,000 rpm for 10 min).

Preparation of water-dispersible Fe₃O₄ NPs. Fe₃O₄-OA NPs was modified with mPEG-COOH to get the water-dispersible Fe₃O₄ NPs. Firstly, 20 mg of mPEG-COOH and 10 mg Fe₃O₄-OA NPs were mixed with 2 ml n-hexane in an eggplant-shaped bottle and sonicated vigorously for 5 min. Then, 5 mL of ultrapure water was added, and sonicated vigorously for 5 min again. After sonication, the n-hexane solvent was removed by rotational evaporation in a water bath at 50 °C. The remaining solution was filtered with a 100 nm aqueous filter to obtain transparent solution with Fe₃O₄-PEG NPs.

Cell culture and cytotoxicity test. The mouse breast cancer cells (4T1) and mouse fibroblasts (3T3) cells were cultured and used in strict accordance with aseptic procedures. The red blood cells used in the hemolysis experiment were obtained from immune deficient BALB/c female mice. The hemolysis experiment operation was performed directly after the cell line was taken out. During recovery, culture, passage, and nanomaterial incubation, the cells were cultured in medium-sized petri dishes. The whole process of the cell growth was carried out in a CO₂ thermostatic incubator at 37 °C. The cytotoxicity test (MTT) of the Fe₃O₄@ZIF-8-Zn-Mn NPs was as follows: 4T1 cells and 3T3 cells were incubated in 96-well plates for 24 h, respectively. Then, Fe₃O₄-Mn-ZIF-8 NPs (0, 5, 10, 20, 50, and 100 µg/mL) were added and the cells were incubated for another 12 or 24 h at 37 °C with 5% CO₂. Next, the upper layer of culture medium was sucked out from the 96-well plate, and then thiazolyl blue tetrazolium bromide (20 µL, 5 mg/mL) was added to each well. The cells were incubated for another 4 h under the similar incubation conditions. Finally, the supernatant of the MTT solution was removed, and the remaining purple formazan crystals were lysed with 150 µL of dimethyl sulfoxide (DMSO). Ultimately, the optical absorption of the formazan was measured with a microplate reader (Multiskan MK3, Thermo Fisher Scientific, Waltham, MA, USA).

In vivo toxicity test. All mice were purchased from Shanghai JieSiJie Laboratory Animal Co.,Ltd., and all the animal experiments strictly abide by animal ethics regulations of Shanghai Normal University. 5-6 weeks old Balb/C female mice without tumor model were selected as the object of *in vivo* toxicity study. The mice were divided into two groups and carried out simultaneously. The mice in the experimental group and the control group were injected with 100 µL Fe₃O₄@ZIF-8-Zn-Mn NPs and 100 µL PBS respectively through the tail vein, respectively. Two weeks later, the above two groups of mice were dissected and the heart, liver, spleen, lung and kidney were taken for hematoxylin and eosin (H&E) staining analysis.

The biodistribution analysis. To determine the metabolism pathway of Fe₃O₄@ZIF-8-Zn-Mn

NPs, the 4 T1 tumor-bearing mice were randomly divided into 12 groups (one control group and three material groups, $n = 3$), and respectively received intravenous injection with $\text{Fe}_3\text{O}_4@\text{ZIF-8-Zn-Mn}$ NPs at different time points (0.5, 1, 2, 4, 8, 12, 24 and 72h), respectively. After that, the mice were sacrificed, and the main organs and metabolites (heart, liver, spleen, lung, kidney, tumor) were collected for ICP analysis of Fe, Mn, Zn content. The distribution of $\text{Fe}_3\text{O}_4@\text{ZIF-8-Zn-Mn}$ NPs was calculated by the injected dose percentage per gram of tissue (% ID/g).

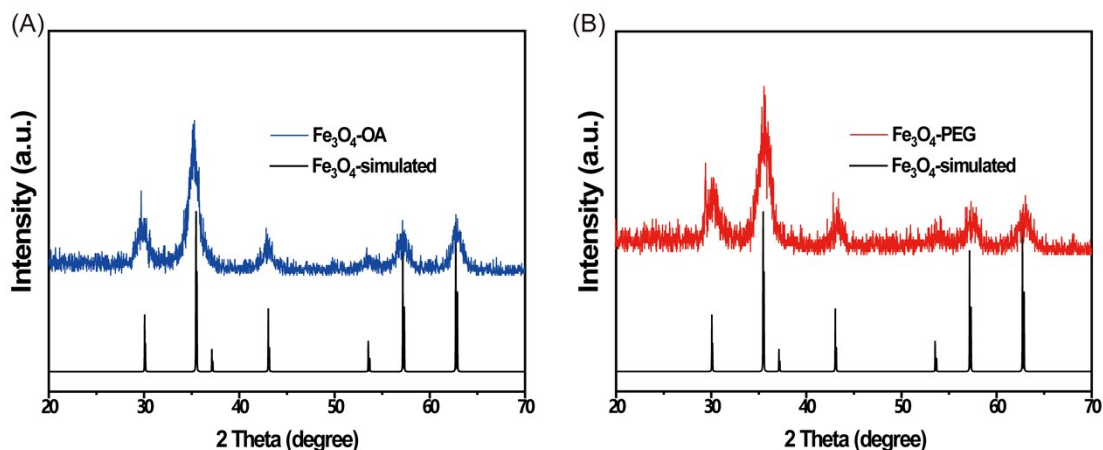


Fig. S1. (A) XRD patterns of $\text{Fe}_3\text{O}_4\text{-OA}$ and $\text{Fe}_3\text{O}_4\text{-simulated}$. (B) XRD patterns of $\text{Fe}_3\text{O}_4\text{-PEG}$ and $\text{Fe}_3\text{O}_4\text{-simulated}$.

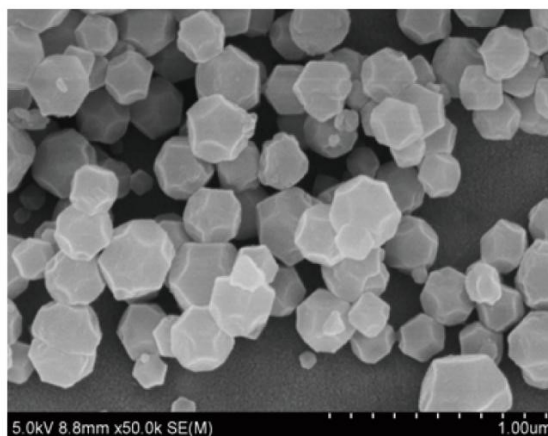


Fig. S2. SEM image of ZIF-8 NPs.

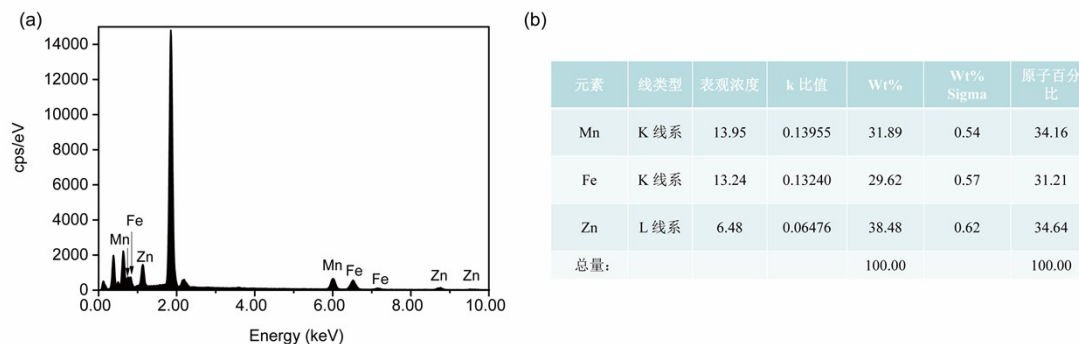


Fig. S3. EDX of the $\text{Fe}_3\text{O}_4@\text{ZIF-8-Zn-Mn}$ NPs.

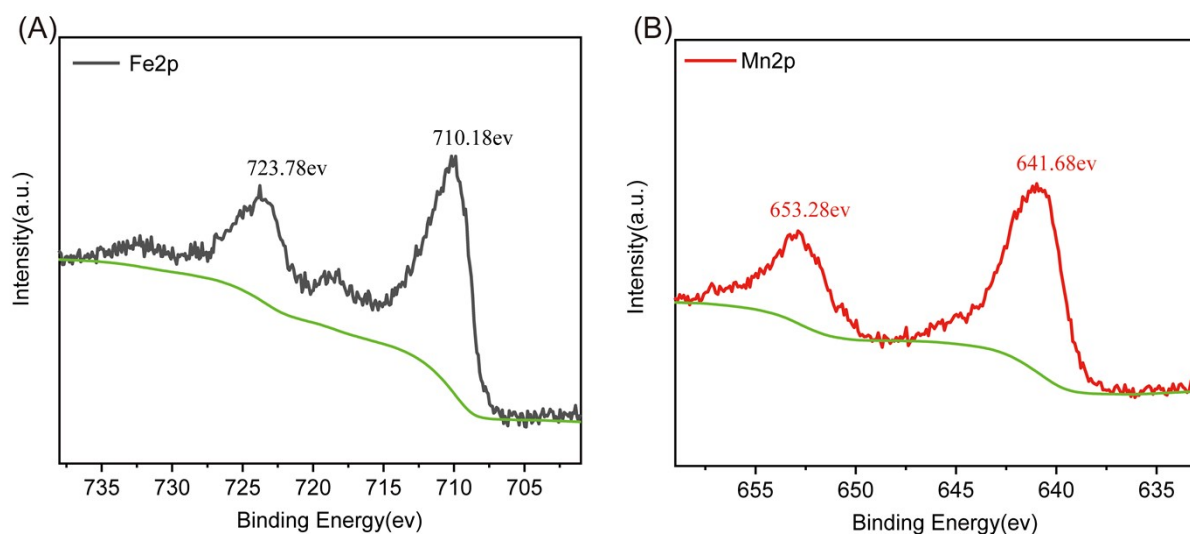


Fig. S4. (A) Mn2p peaks and (B) Fe2p peaks of $\text{Fe}_3\text{O}_4@\text{ZIF-8-Zn-Mn}$ NPs.

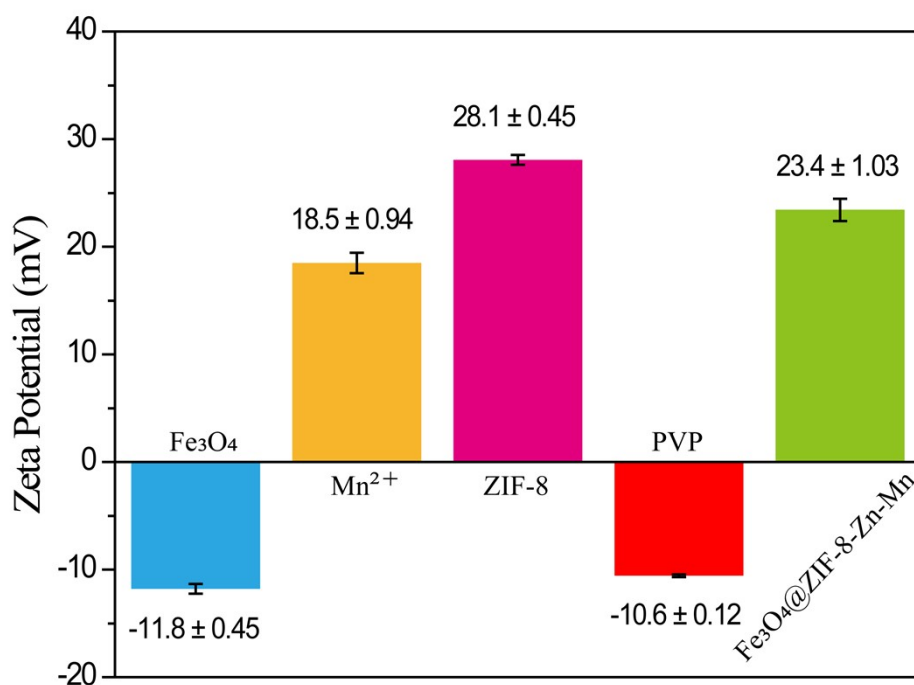


Fig. S5. Zeta Potential of the water-soluble $\text{Fe}_3\text{O}_4\text{-PEG}$, $\text{Mn}(\text{NO}_3)_2 \cdot 4\text{H}_2\text{O}$, ZIF-8, PVP and $\text{Fe}_3\text{O}_4@\text{ZIF-8-Zn-Mn}$ NPs.

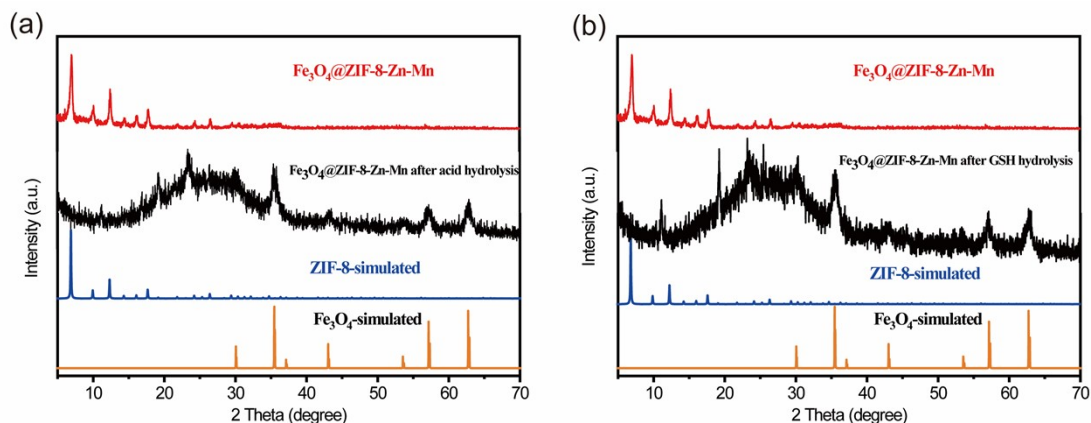


Fig. S6. XRD patterns of (a) $\text{Fe}_3\text{O}_4@\text{ZIF-8-Zn-Mn}$ after acid hydrolysis, (b) $\text{Fe}_3\text{O}_4@\text{ZIF-8-Zn-Mn}$ after GSH hydrolysis.

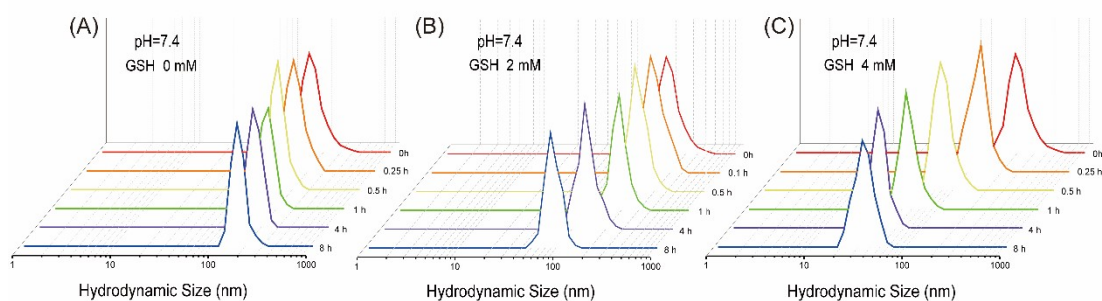


Fig. S7 Temporal hydrodynamic size profiles of $\text{Fe}_3\text{O}_4@\text{ZIF-8-Zn-Mn}$ NPs in Tris-HCl buffer solution with (A) pH of 7.4 without GSH, (B) pH of 7.4 and 2 mM GSH and (C) pH of 7.4 and 4 mM GSH.

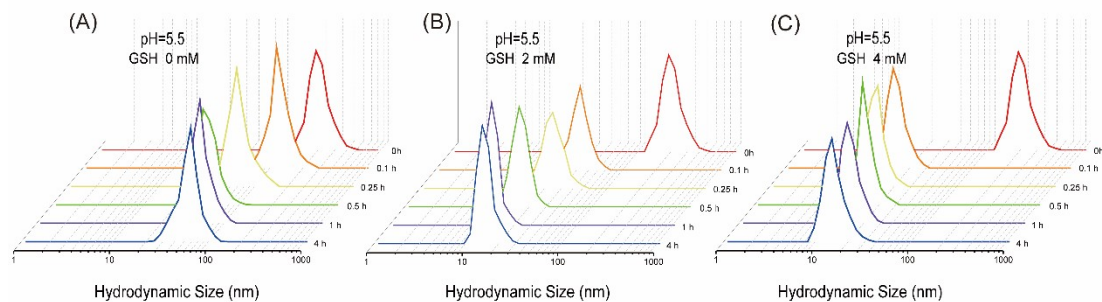


Fig. S8 Temporal hydrodynamic size profiles of $\text{Fe}_3\text{O}_4@\text{ZIF-8-Zn-Mn}$ NPs in Tris-HCl buffer solution with (A) pH of 5.5 without GSH, (B) pH of 5.5 and 2 mM GSH and (C) pH of 5.5 and 4 mM GSH.

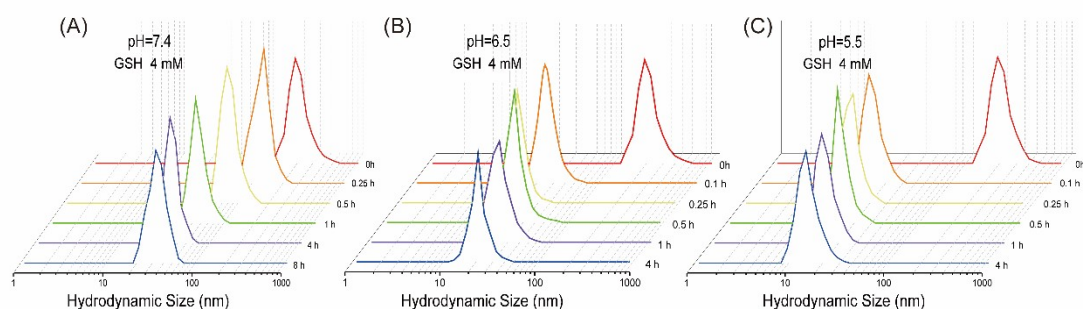


Fig. S9 Temporal hydrodynamic size profiles of $\text{Fe}_3\text{O}_4@\text{ZIF-8-Zn-Mn}$ NPs in Tris-HCl buffer solution with (A) pH of 7.4 and 4mM GSH, (B) pH of 6.5 and 4 mM GSH and (C) pH of 5.5 and 4 mM GSH.

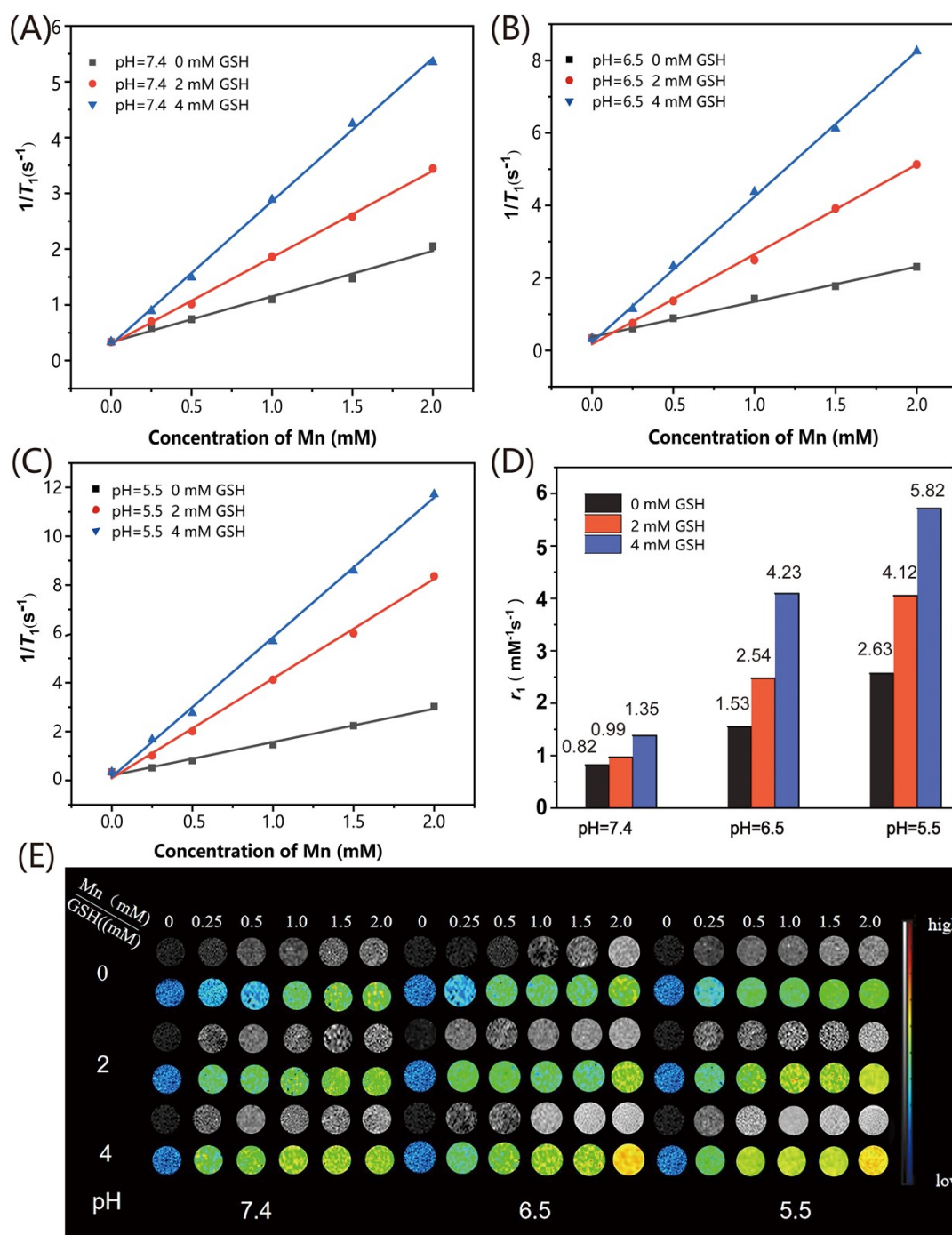


Fig. S10 T_1 -weighted MRI of $\text{Fe}_3\text{O}_4@\text{ZIF-8-Zn-Mn}$ NPs under 0.5 T magnetic field. Relaxation rates of $\text{Fe}_3\text{O}_4@\text{ZIF-8-Zn-Mn}$ NPs in Tris-HCl buffer solution with (A) pH=7.4, (B) pH=6.5 and (C) pH=5.5 and different concentrations of GSH (0-4 mM). (D) Corresponding r_1 relaxation rate values and (e) T_1 -weighted MRI images under different pH and GSH concentrations.

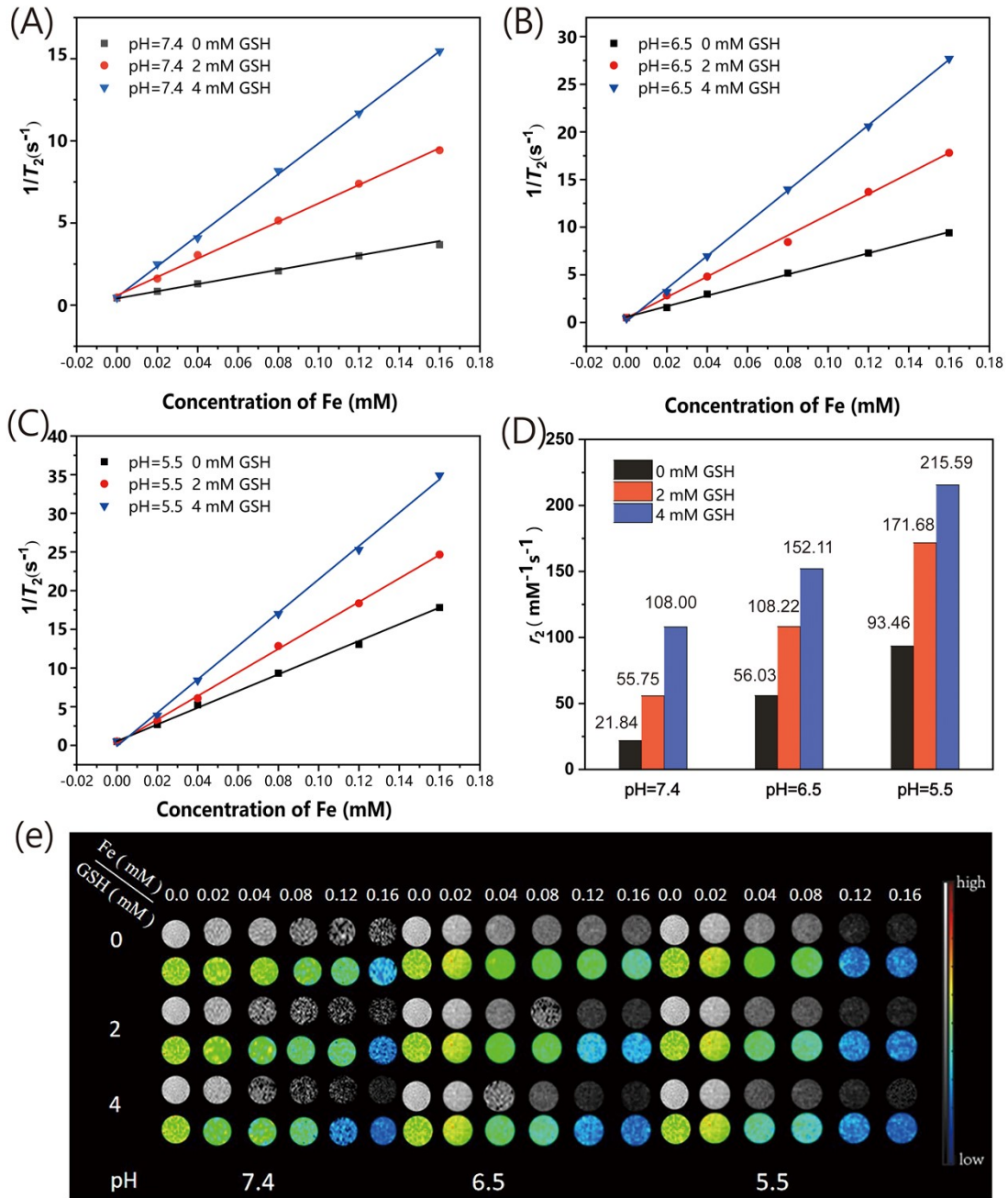


Fig. S11 T_2 -weighted MRI of $\text{Fe}_3\text{O}_4@ZIF-8\text{-Zn-Mn}$ NPs under 0.5 T magnetic field. Relaxation rates of $\text{Fe}_3\text{O}_4@ZIF-8\text{-Zn-Mn}$ NPs in Tris-HCl buffer solution with (A) pH=7.4, (B) pH=6.5 and (C) pH=5.5 and different concentrations of GSH (0-4 mM). (D) Corresponding r_2 relaxation rate values and (E) T_2 -weighted MRI images under different pH and GSH concentrations.

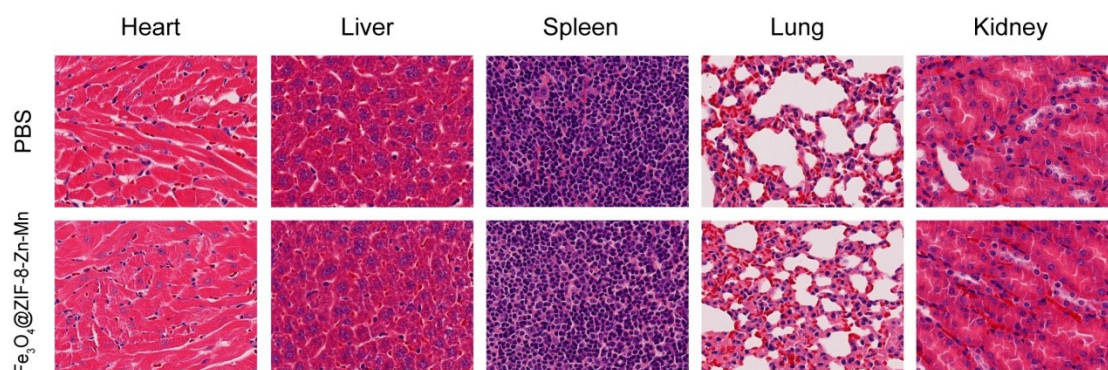


Fig. S12 H&E staining of major organs of mice after the injection of PBS and $\text{Fe}_3\text{O}_4@\text{ZIF-8-Zn-Mn}$ NPs for two weeks.

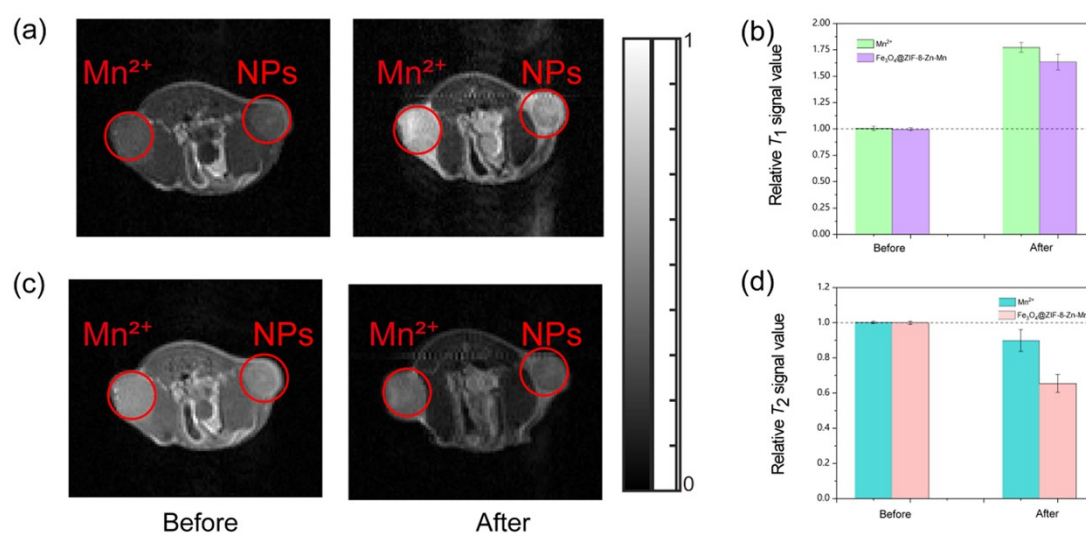


Fig. S13 Magnetic resonance imaging study in bilateral tumor-bearing mice models (intratumor injection of NPs) under 1 T magnetic field. (a) T_1 -weighted imaging and (b) corresponding relative imaging signal intensity of the tumor sites before and after intratumor injection of Mn^{2+} and $\text{Fe}_3\text{O}_4@\text{ZIF-8-Zn-Mn}$ NPs; (c) T_2 -weighted imaging and (d) corresponding relative imaging signal intensity of the tumor sites before and after intratumor injection of Mn^{2+} and $\text{Fe}_3\text{O}_4@\text{ZIF-8-Zn-Mn}$ NPs.

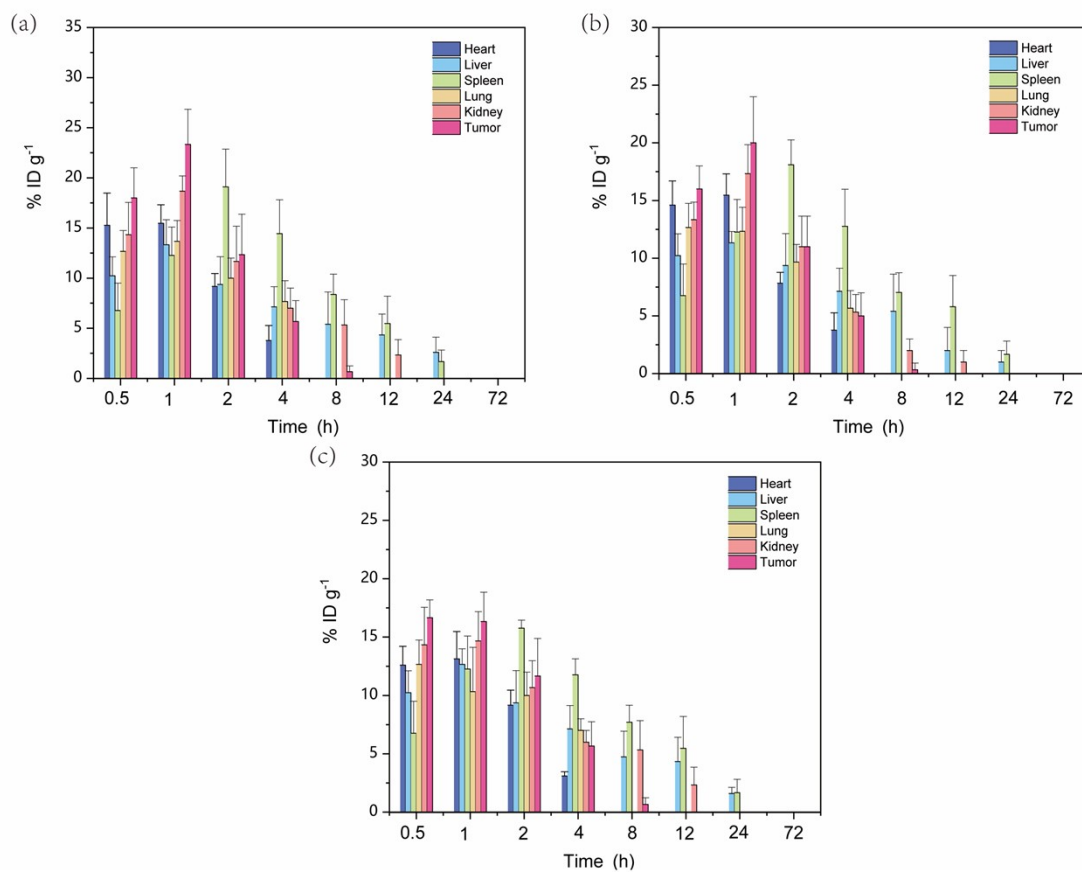


Fig. S14 Time-dependent biodistribution of the Zn, Fe and Mn of the Fe₃O₄@ZIF-8-Zn-Mn NPs in main 6 organs, tumors.